

AD-A066 827

TEXAS UNIV AT AUSTIN APPLIED RESEARCH LABS

QUARTERLY PROGRESS REPORT NUMBER 3, 5 JULY-5 OCTOBER 1970.(U)

OCT 70

F/G 17/1

N00024-70-C-1184

NL

UNCLASSIFIED

| OF |
AD
AD 66827



END
DATE
FILED

5-79

DDC

AD A0 66827

000995

LEVEL II
871434 OPR 2

1

007 LIBRARY COPY

APPLIED
RESEARCH
LABORATORIES
THE UNIVERSITY OF TEXAS
AT AUSTIN

Good

7 MOST Project

-3

26 October 1970

Copy No. 2

QUARTERLY PROGRESS REPORT NO. 3

CONTRACT N00024-70-C-1184

5 July - 5 October 1970

NAVAL SHIP SYSTEMS COMMAND
Contract N00024-70-C-1184
Proj. Ser. No. SF 11121103, Task 8614

007 FILE COPY

000995

007 LIBRARY COPY



DISTRIBUTION STATEMENT A

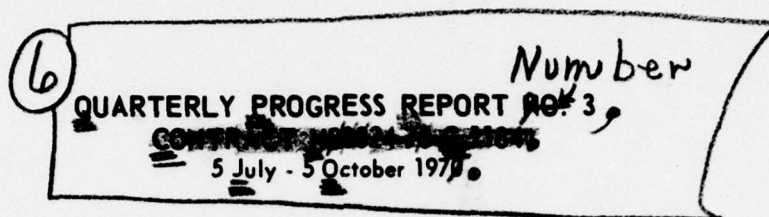
Approved for public release;
Distribution Unlimited

For Official Use Only

2009010

This document is subject to special export control
and each transmission to foreign governments or
foreign nationals may be made only with prior approval
of NAVSHIPS OVICOS

(11) 26 Oct 1970



(15) N00024-70-C-1184

(12) 29 pi

NAVAL SHIP SYSTEMS COMMAND
Contract N00024-70-C-1184
Proj. Ser. No. SF 11121103, Task 8614

ACCESSION FOR	
NTIS	White Section
DDC	Buff Section <input type="checkbox"/>
CHANGING	
JUSTIFICATION	
Radar on file	
BY	
DISTRIBUTION/AVAILABILITY CODES	
Distr.	Avail. Exch/N Spec
A	

(16) F11121

(17) SF11121103

This document is subject to special export control
and shall not be furnished to foreign governments.
Foreign nationals may be made only with prior approval
NAVSUPPLIES DIVISION

APPLIED RESEARCH LABORATORIES
THE UNIVERSITY OF TEXAS AT AUSTIN
AUSTIN, TEXAS 78712

~~For Official Use Only~~

DISTRIBUTION STATEMENT A
Approved for public release;
Distribution Unlimited

404 434

Alt

TABLE OF CONTENTS

	<u>Page</u>
I. INTRODUCTION	1
II. SIGNAL PROCESSING	3
III. STATISTICAL ANALYSIS	5
IV. PROCESSING GAIN	17
V. COMMENTS	23
APPENDIX I	25
REFERENCES	29

I. INTRODUCTION

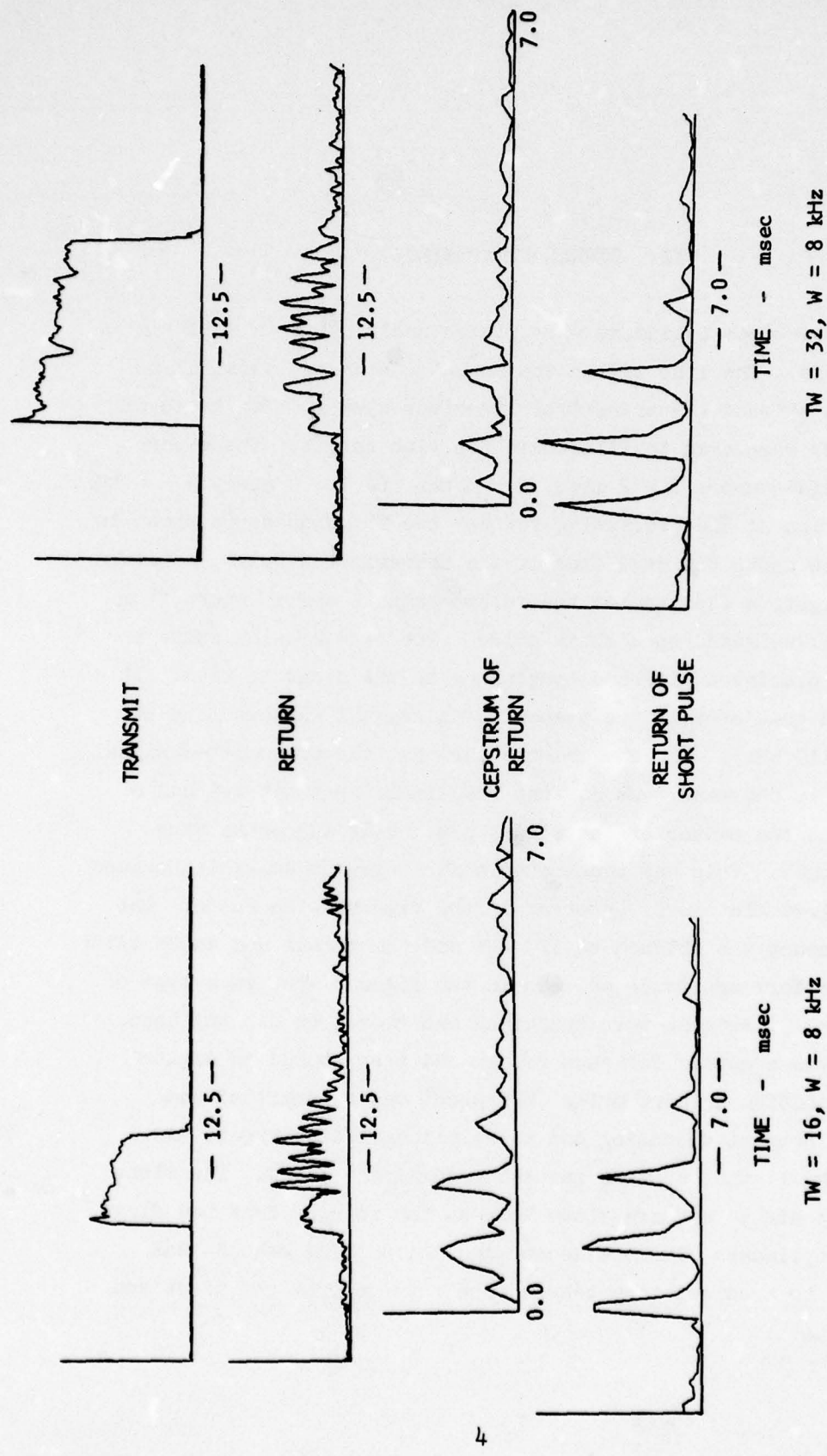
During the previous quarter, several sets of sonar sea data were quantized and stored on digital tape. These data represented five different transmission modes and it was intended to use these data for a statistical study of cepstrum analysis. At that time the cepstrums that were produced showed very poor results and the statistical study was delayed until a reason could be found to explain the poor results. It was speculated that several reasons might account for the poor results: one reason might have been programming errors and another reason might have been poor data.

Cepstrum analysis During the present quarter an effort has been made to explain *the problems with these problems*. A carefully controlled experiment was conducted at the Applied Research Laboratories Lake Travis Test Station, using three styrofoam cylinders as a target. The transmission and return signals were recorded on analog tape and returned to the laboratory. The signals were then quantized and stored on digital tape for later analysis. The results of that analysis are included in this report.

In addition, a study using artificially generated data was used to calculate the processing gain of cepstrum. This was compared with the processing gain for a replica correlator and an autocorrelator. The results of this study are important and they are shown at the end of the report.

II. SIGNAL PROCESSING

Three styrofoam cylinders were placed under water in a line at a depth of 10 ft. The line was in the acoustic beam and parallel to the acoustic axis of the transmitter/receiver system. Two types of transmissions were used to illuminate the line target. These were linear FM slides where $T = 2$ msec, $W = 8$ kHz and $T = 4$ msec, $W = 8$ kHz. An illustration of the processing for the two TW products is shown in Fig. 1. This shows the envelopes of the transmission pulse, a return from the target, a cepstrum of the return signal, and a return from the target illuminated by a short pulse. The transmission pulse was recorded by placing a wideband hydrophone in the acoustic beam. It was observed that usually the transmitting crystal was operated at resonance (110 kHz). The consequence was that the transmitted signal as recorded in the water was no longer a linear FM slide but had a large peak in the center of the slide, plus nulls and peaks very near its center. This was unacceptable for cepstrum analysis because of the required flat power spectrum in the transmission pulse. The center frequency was shifted to 125 kHz and the result was an FM slide of almost uniform amplitude as seen in the figure. For each type of transmission, 90 returns were quantized and stored on digital tape. A cepstrum was computed for each return and also stored on digital tape. In addition a short pulse (200 μ sec) was transmitted and recorded to help with scaling and to help locate the target. As shown in Fig. 1, the cepstrum has two predominant peaks. The first peak corresponds to a correlation between the returns from the first and second cylinders plus the second and third. The second peak corresponds to a correlation between the returns from the first and third cylinders.



AS-70-1327

FIGURE 1
SIGNAL PROCESSING ON THE RETURN FROM A 3 POINT TARGET

III. STATISTICAL ANALYSIS

It was shown in Quarterly Progress Report No. 1 that the x,y quadrature components of the cepstrum can be averaged to obtain a processing gain in the presence of a stable target plus noise. The envelopes of averaged cepstrums are shown in Figs. 2 through 5. Each envelope is the average of three cepstrums and when they are compared with Fig. 1, it is clear that a processing gain has been achieved. It is also clear that the averages are fairly consistent, but there are changes with time. The changes are attributed to the fact that the cylinders are moving with respect to each other from ping to ping. This means that if too many cepstrums are averaged together, the peaks in the cepstrum that indicate the presence of a target can be obscured. A point is now raised, which will have to be settled later, concerning the practicality of averaging the x,y quadrature components versus averaging the envelopes. The covariance matrix of the cepstrums for the two TW products is shown in Fig. 6. In the quadrature formulation the covariance matrix is

$$\begin{aligned} \text{Cov}(\tau_i, \tau_j) &= \sum_{k=1}^{90} (x_i^k x_j^k + y_i^k y_j^k) \cos \omega_o (\tau_i - \tau_j) \\ &\quad + \sum_{k=1}^{90} (x_i^k y_j^k - x_j^k y_i^k) \sin \omega_o (\tau_i - \tau_j) , \end{aligned} \tag{1}$$

and the figures plotted are actually the magnitudes of the covariance matrix. The subscripts i, j refer to the lag times of the cepstrum and

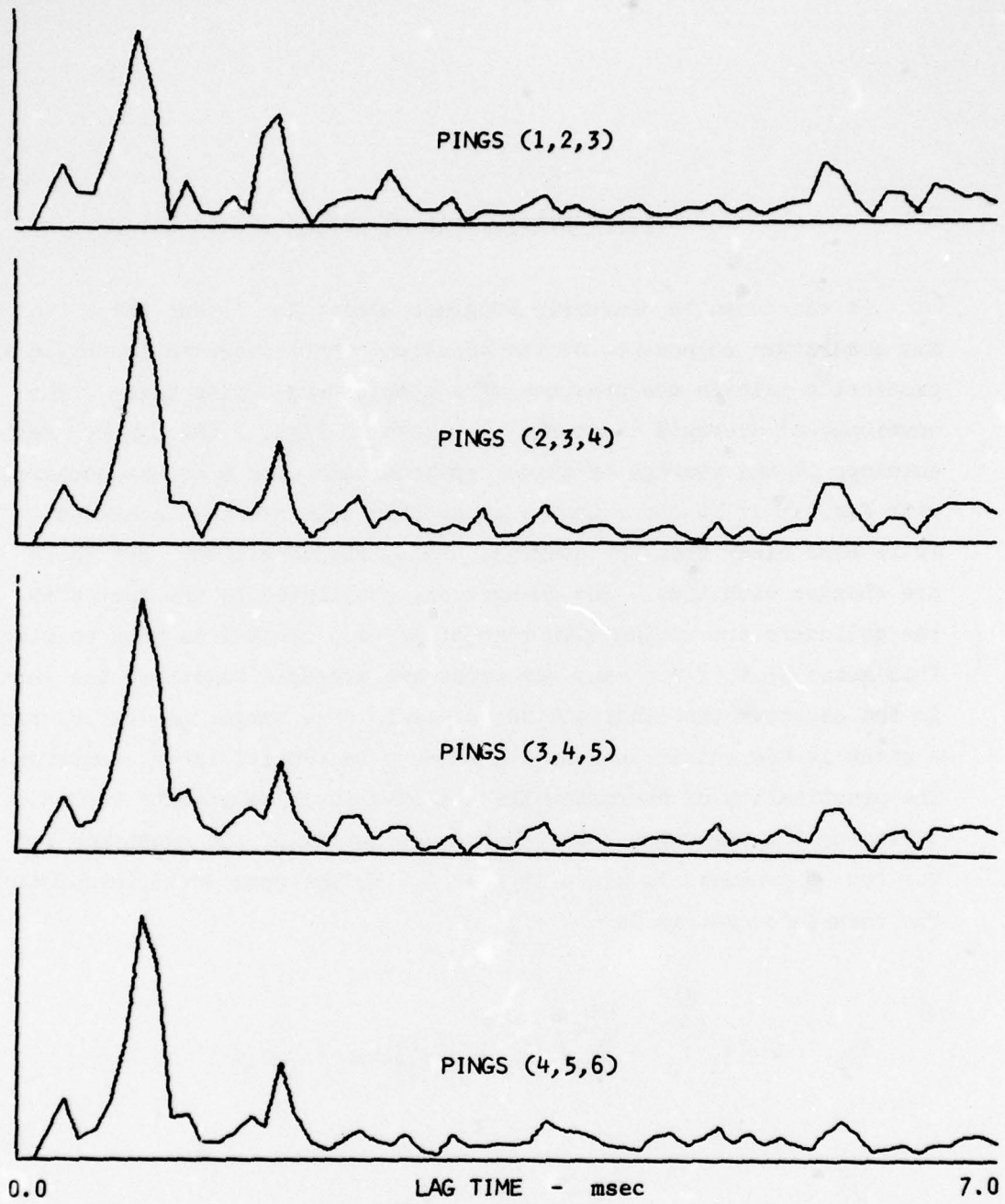


FIGURE 2
AVERAGED CEPSTRUMS FOR A 3 POINT TARGET
 $TW = 16$, $W = 8$ kHz

AS-70-1328

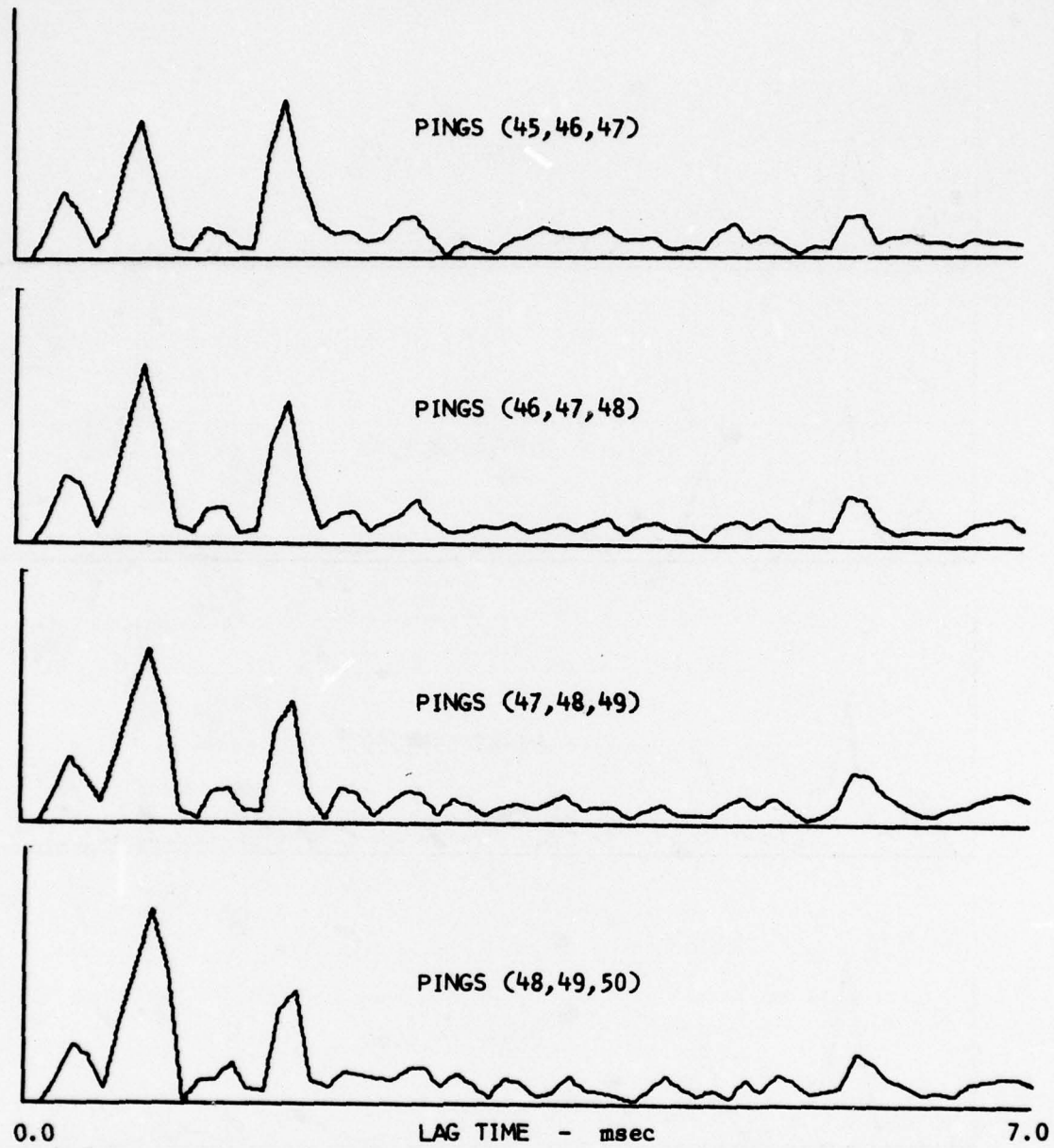


FIGURE 3
AVERAGED CEPSTRUMS FOR A 3 POINT TARGET
 $T_W = 16$, $W = 8$ kHz

AS-70-1329

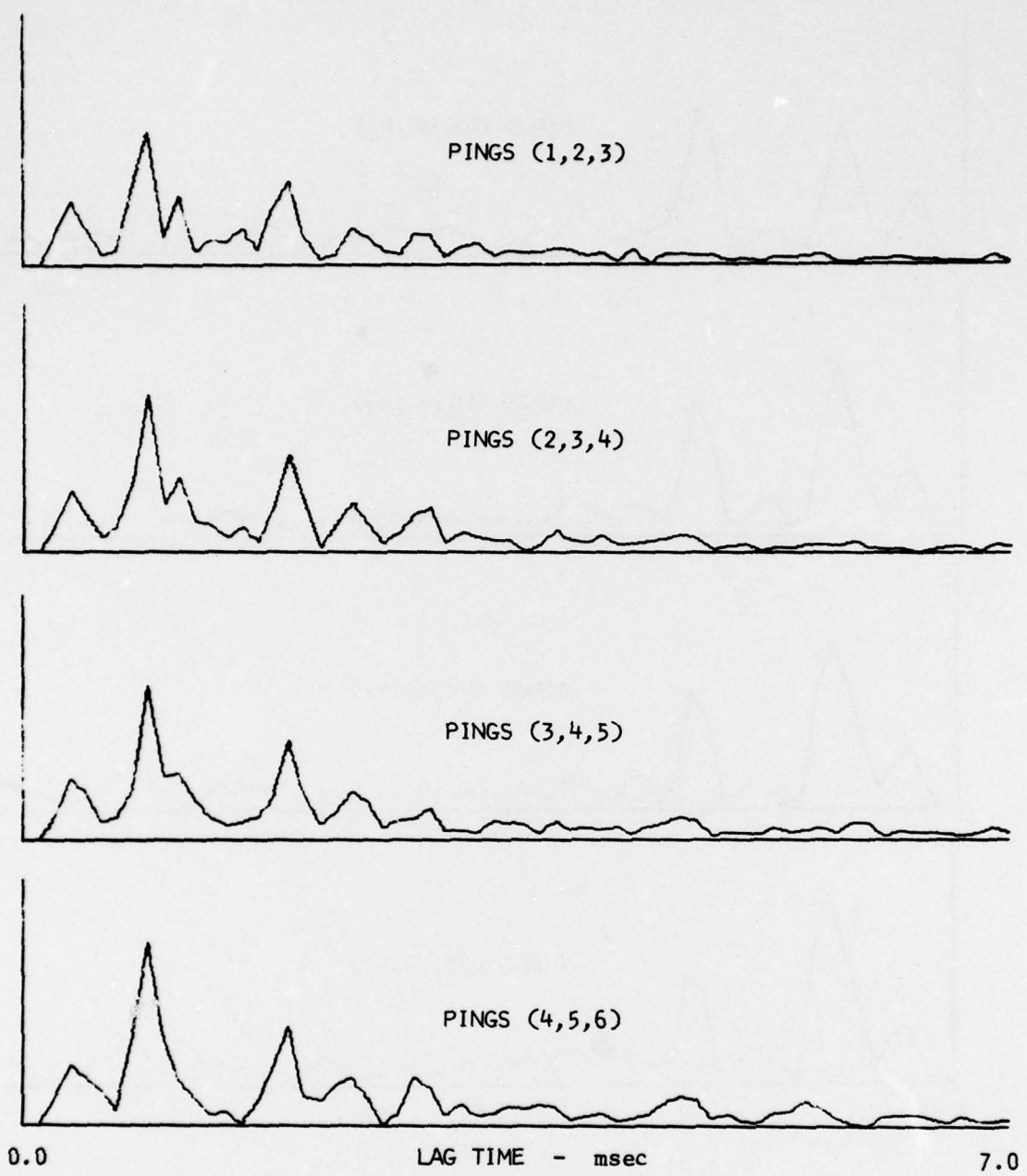


FIGURE 4
AVERAGED CEPSTRUMS FOR A 3 POINT TARGET
 $TW = 32$, $W = 8$ kHz

AS-70-1330

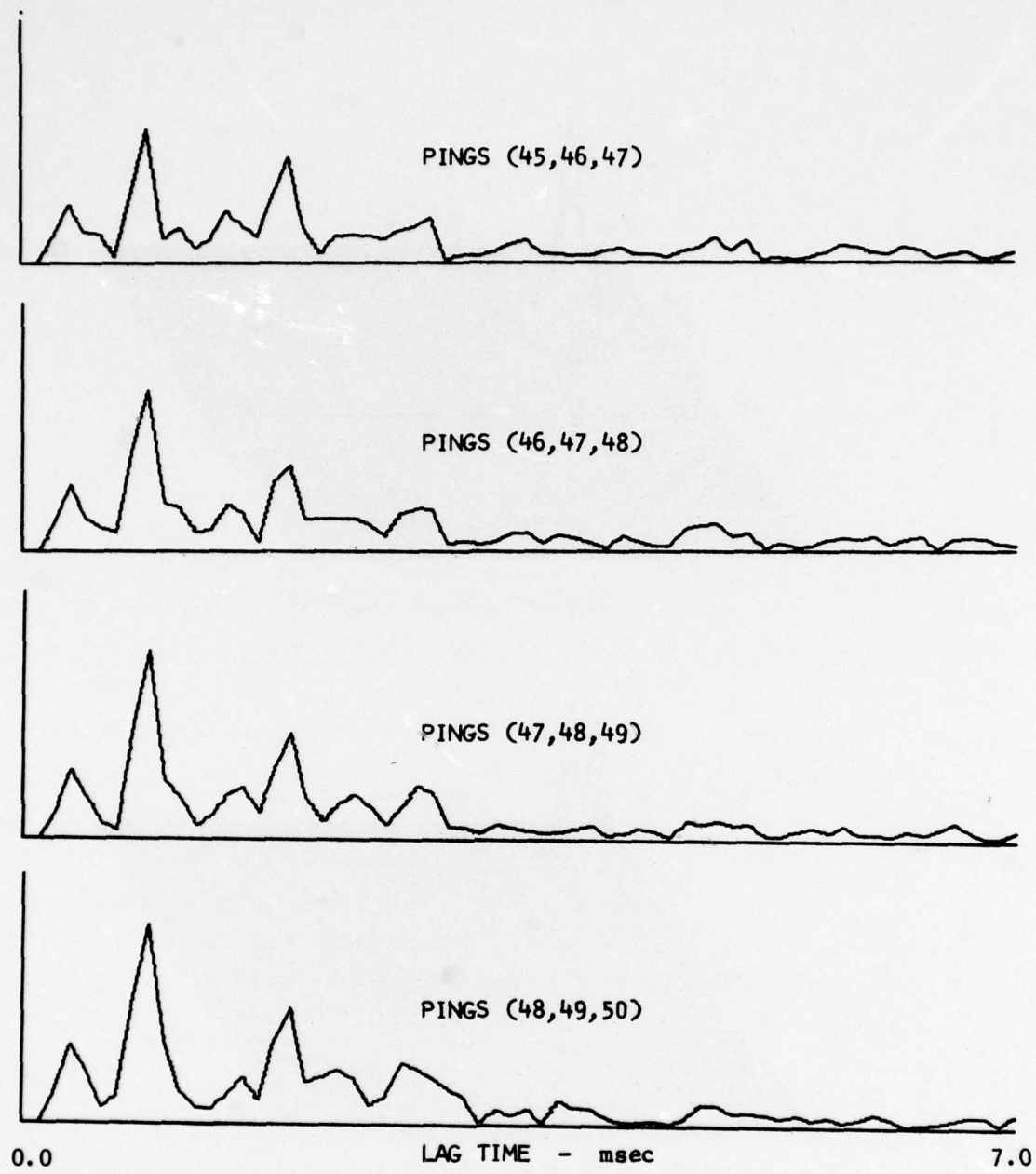


FIGURE 5
AVERAGED CEPSTRUMS FOR A 3 POINT TARGET
 $TW = 32$, $W = 8$ kHz

AS-70-1331

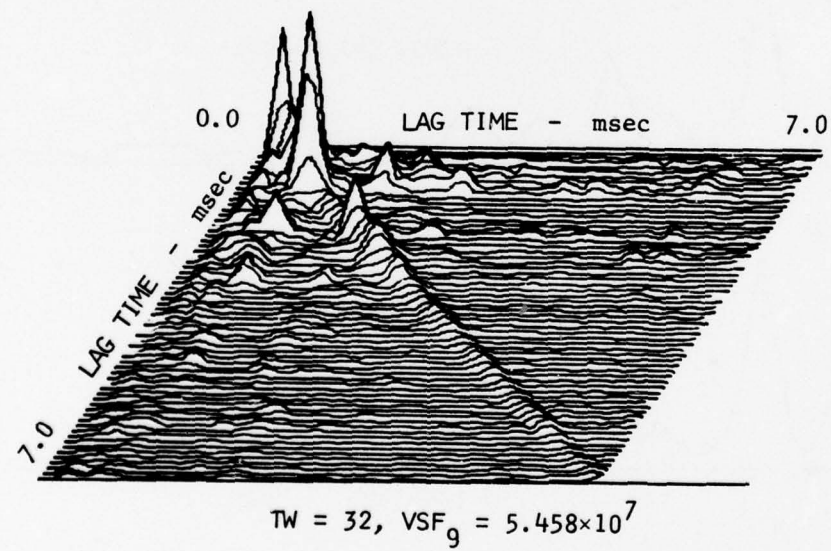
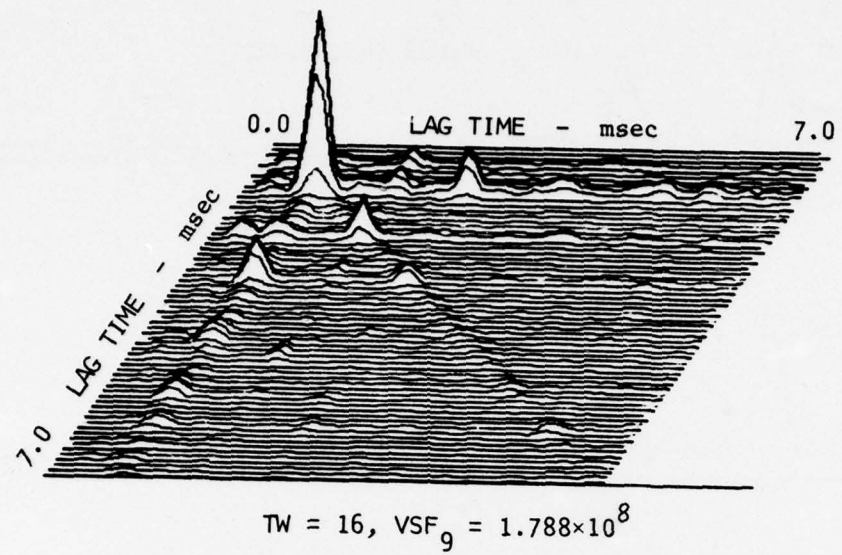


FIGURE 6
CEPSTRUM COVARIANCE MATRIX FOR A 3 POINT TARGET

the superscript k refers to the ping numbers. The main diagonal of the matrix corresponds to the square of the average envelope and it appears that in this case the average of the envelopes gives an excellent result. That is to say, the expected peaks are large with respect to the surrounding noise. The peaks off of the main diagonal are correlations between the two primary peaks. It will be noted that the matrix is Hermitian, which is to say that

$$|\text{Cov}(\tau_i, \tau_j)| = |\text{Cov}(\tau_j, \tau_i)| , \quad (2)$$

or that it is symmetrical about the main diagonal. The upper left-hand corner of the matrix corresponds to the origin at lag time 0,0. The lower right-hand corner corresponds to 7 msec, 7 msec. This is exactly the same time scale shown in Figs. 2 through 5.

To gain further insight into the statistical nature of the cepstrum, the x components were tested for independence, homogeneity, and for particular probability densities.¹ This was done by hypothesis testing. For example, in the test for independence it is assumed that the data are independent, which is referred to as the null hypothesis (H_0). Then a one sample runs test is used to generate a test statistic (number of runs) which has a known probability distribution given H_0 . If H_0 is true, then the test statistic, which is a random variable, will fall below a certain threshold with a certain probability, and a decision can be made in regard to the independence at a confidence level equal to the specified probability. In the particular tests to be shown, a data set (S_i) consists of the samples

$$S_i = \left\{ x_i^k \mid i = \text{constant}, k = 1, 2, \dots, 90 \right\} , \quad (3)$$

which would correspond to samples taken from a vertical cross section of Fig. 2. Again it is mentioned that the subscript i refers to a lag time, τ_i . In the runs test, consecutive values of S_i of the same sign constitute a run, and zeroes are ignored. The test statistic is the number of runs and for a large number of samples the probability density of the test statistic is a normal distribution, given that H_0 is true.

By homogeneity one means that the data samples in the set, S_i , are all generated by the same statistical mechanism. The test statistic in this case is generated by subdividing S_i , obtaining the cumulative probability distributions of each subset, and then finding the maximum differences between the cumulative probability distributions. Given H_0 , the test statistic (maximum difference) is Smirnov distributed and this test is referred to as the Kolmogorov-Smirnov two sample test. In the particular test to be shown, the data sets were divided into halves.

The two sample test can be extended to test for a theoretical probability distribution. The difference is that the data sample is tested against a theoretical distribution instead of against a subset of itself. This is referred to as the Kolmogorov-Smirnov one sample test.

The results of these tests are shown in Figs. 7 and 8 for the two TW products. In each of the graphs the statistic is plotted versus lag time, τ_i . All of the tests are independent of the magnitude of the samples (nonparametric). Threshold lines are drawn for 50% and 95% confidence levels. Usually when the statistics fall above the 95% level, the null hypothesis H_0 is rejected. It is seen from the test for independence that there is a significant number of rejections, especially in the region around the principal peaks in

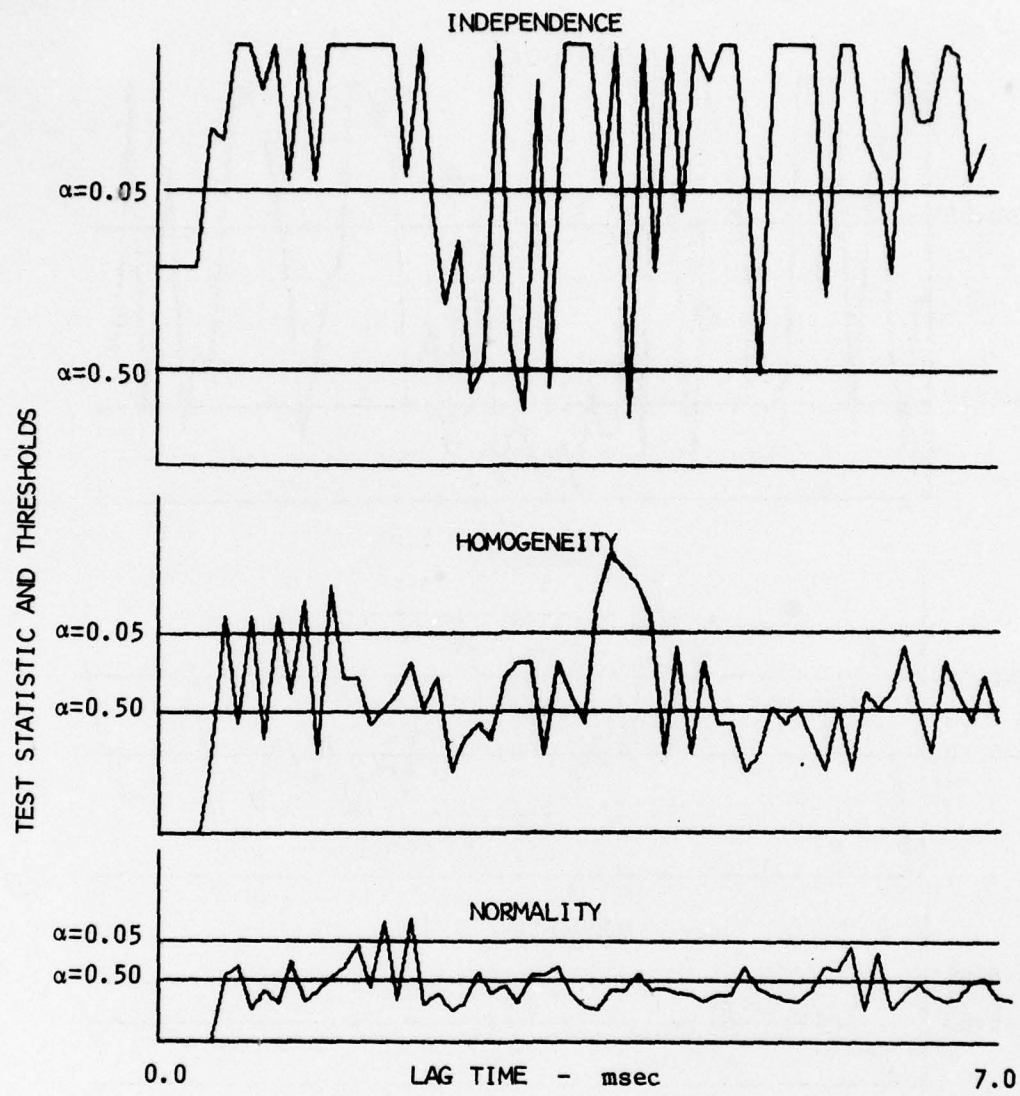


FIGURE 7
STATISTICAL TESTS ON x-QUADRATURE COMPONENT
OF THE CEPSTRUMS OF A 3 POINT TARGET
 $TW = 16$, $W = 8$ kHz

AS-70-1333

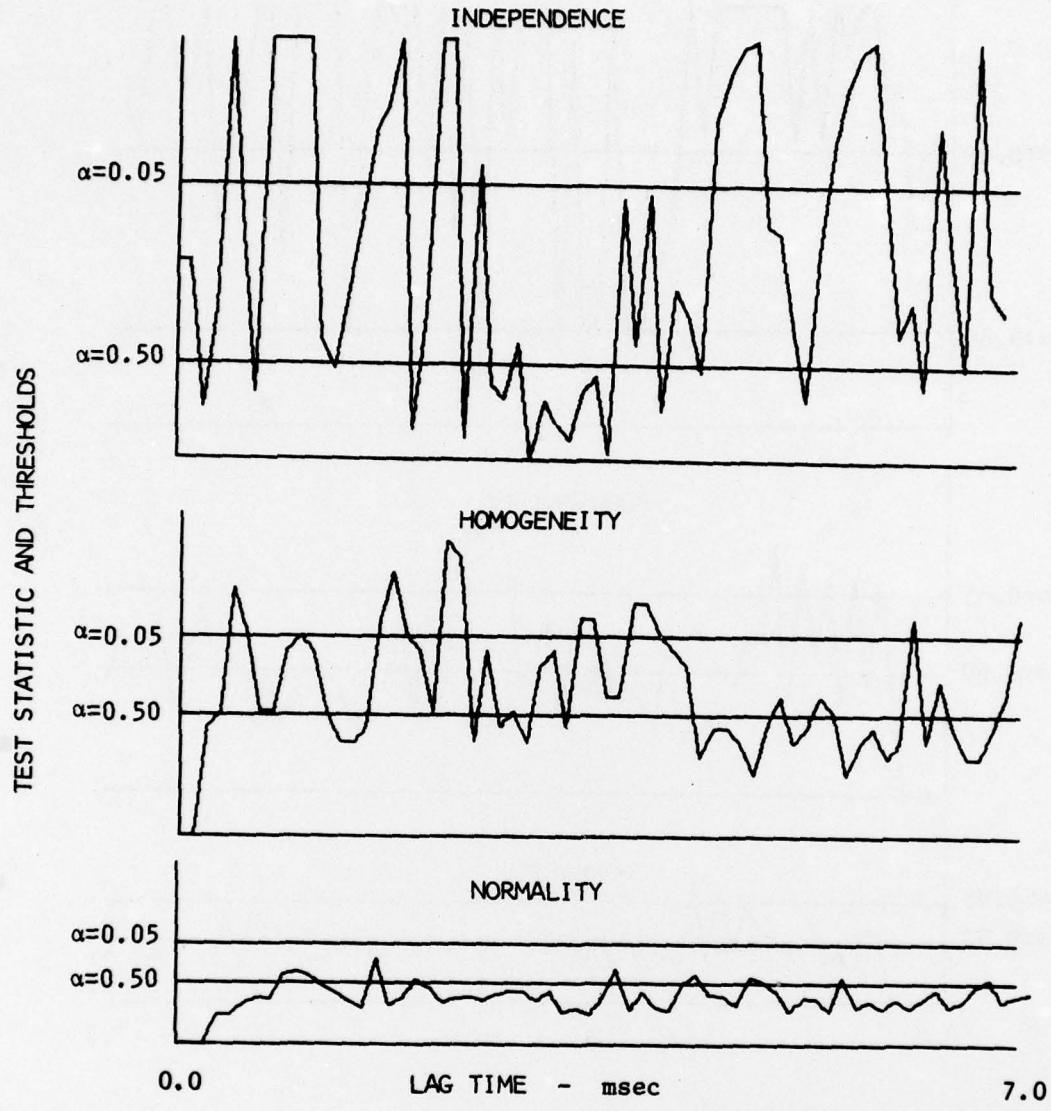


FIGURE 8
 STATISTICAL TESTS ON x-QUADRATURE COMPONENT
 OF THE CEPSTRUMS OF A 3 POINT TARGET
 $TW = 32$, $W = 8$ kHz

AS-70-1334

the cepstrum. This is not surprising because it already is known that the x,y components can be averaged to obtain a processing gain. However, it is discouraging to see many rejections at lag times greater than, say, 2.5 msec. Perhaps a parametric test would be more suitable here to obtain the significance of this result. It would be concluded from this result that the data samples are random variables, but they are not independent. The results of the test for homogeneity are marginal. It appears that there might be trends in the data causing the data samples to appear to be generated by different mechanisms. On the whole one would accept the data to be homogeneous. Given that the data is homogeneous, one naturally wishes to know the type of probability distribution. The data were tested for normal, Cauchy, uniform, exponential, Raleigh, and Poisson probability densities. Except for normality, all of the hypotheses were rejected. The tests for normality are shown in the Figs. 7 and 8.

IV. PROCESSING GAIN

A significant part in the study of applying cepstrum to active sonar is to determine its processing gain. For this purpose cepstrum is thought of as a black box with a certain signal-to-noise ratio on its input and a corresponding signal-to-noise ratio on its output. The processing gain, G , is then the ratio of the output-to-input ratios. That is

$$G = \frac{\text{Peak}(S+N)_o^2 / N_o}{(S+N)_{in} / N_{in}} , \quad (4)$$

where

$\text{Peak}(S+N)_o^2$ = peak signal plus noise out squared,

N_o = mean square noise out,

$(S+N)_{in}$ = mean square signal plus noise in,

N_{in} = mean square noise in.

This is a variation of the definition given by Steward and Westerfield² and it will be seen that G is a function of S_{in}/N_{in} . Using artificially generated data, G was numerically computed as a function of S_{in}/N_{in} for three different processors and Fig. 9 shows the result for a time bandwidth product, $TW=16$. It will be noted that the abscissa of Fig. 9 is S/N and not $(S+N)/N$. The results of Fig. 9 can be explained in the following way. The processor for the replica correlator is a crosscorrelation between a replica of the transmitted signal and the received signal. As $S/N \rightarrow \infty$, the definition given by Eq. 4 approaches

18

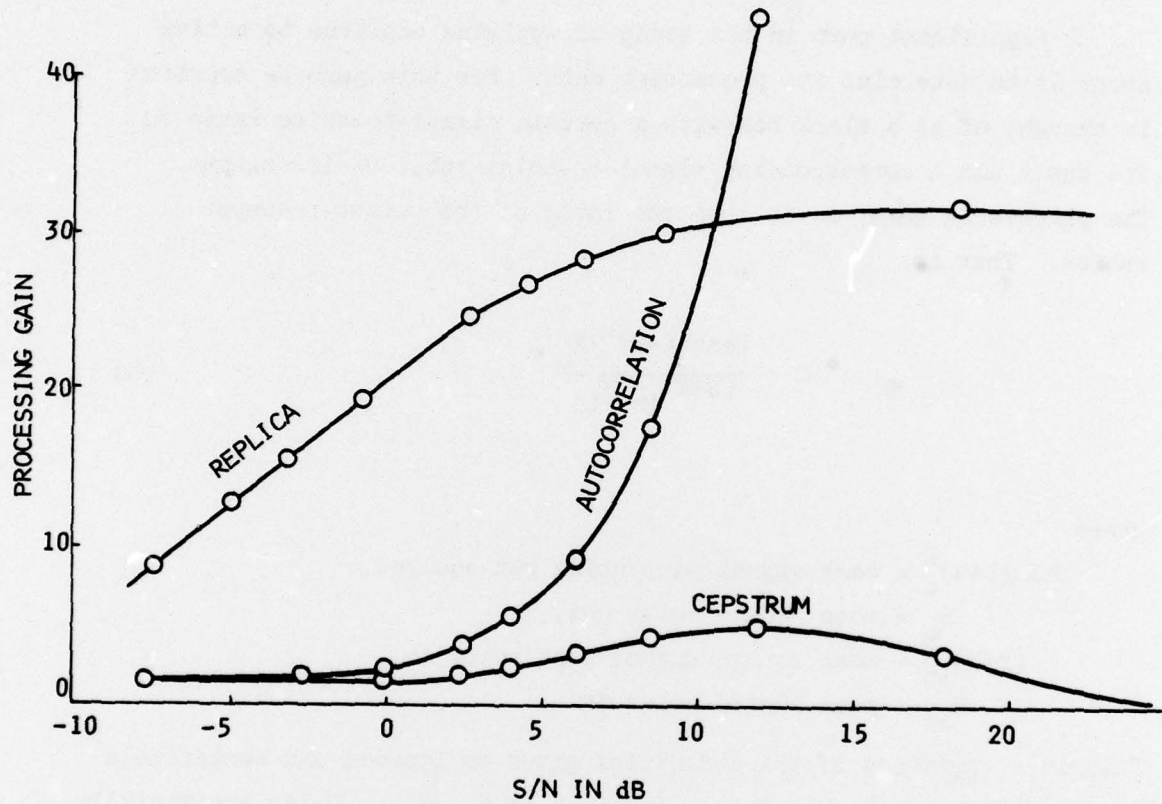


FIGURE 9

THREE PROCESSING GAINS FOR
 $TW = 16$

AS-70-1340

the definition given by Steward and Westerfield*. In this case, $G=2TW$, which is shown in the figure. In the case of $S/N \rightarrow 0$, it is clear that the noise will dominate and G will approach a constant equal to two.

The results for the autocorrelation and the cepstrum require an explanation of the procedure used in the calculation. The primary point of interest is to be able to detect the time difference between two received replicas of the transmitted signal superimposed in a noise background, as shown in Fig. 10(a). The autocorrelation of Fig. 10(a) is shown in Fig. 10(b), and the cepstrum of Fig. 10(a) is shown in Fig. 10(c). The processing gain is computed by repeating the experiment 10 times and averaging to get the peak $S+N$ out squared. The process is repeated for noise only and typical results are shown in Fig. 11. The G for the autocorrelation grows as the square once the peak signal plus noise out is greater than the surrounding mean square noise out. In the case of the cepstrum the mean square output is independent of the signal amplitude, and as $S_{in}/N_{in} \rightarrow \infty$, the G goes to zero. This is explained more fully in the appendix. It would appear from Figs. 10(b) and 10(c) that the processing gains for autocorrelation and cepstrum are the same. This is not true because the autocorrelation is magnitude dependent, which can be seen by comparing the scales in Fig. 10(b) and Fig. 11(a), which are the autocorrelation outputs for $S+N$ and N only. It is observed that the mean square noise out is smaller than the mean square signal plus noise out. This accounts for the fact that G is greater for the autocorrelation than it is for the cepstrum. The processing gain G is also a function of the TW product and Fig. 12 shows a family of G 's for various TW 's and S_{in}/N_{in} ratios. It is clear that the G increases with TW , as would be expected.

$$G = \frac{\text{Peak}(S)^2 / N_o}{S/N} \text{ as } S/N \rightarrow \infty$$

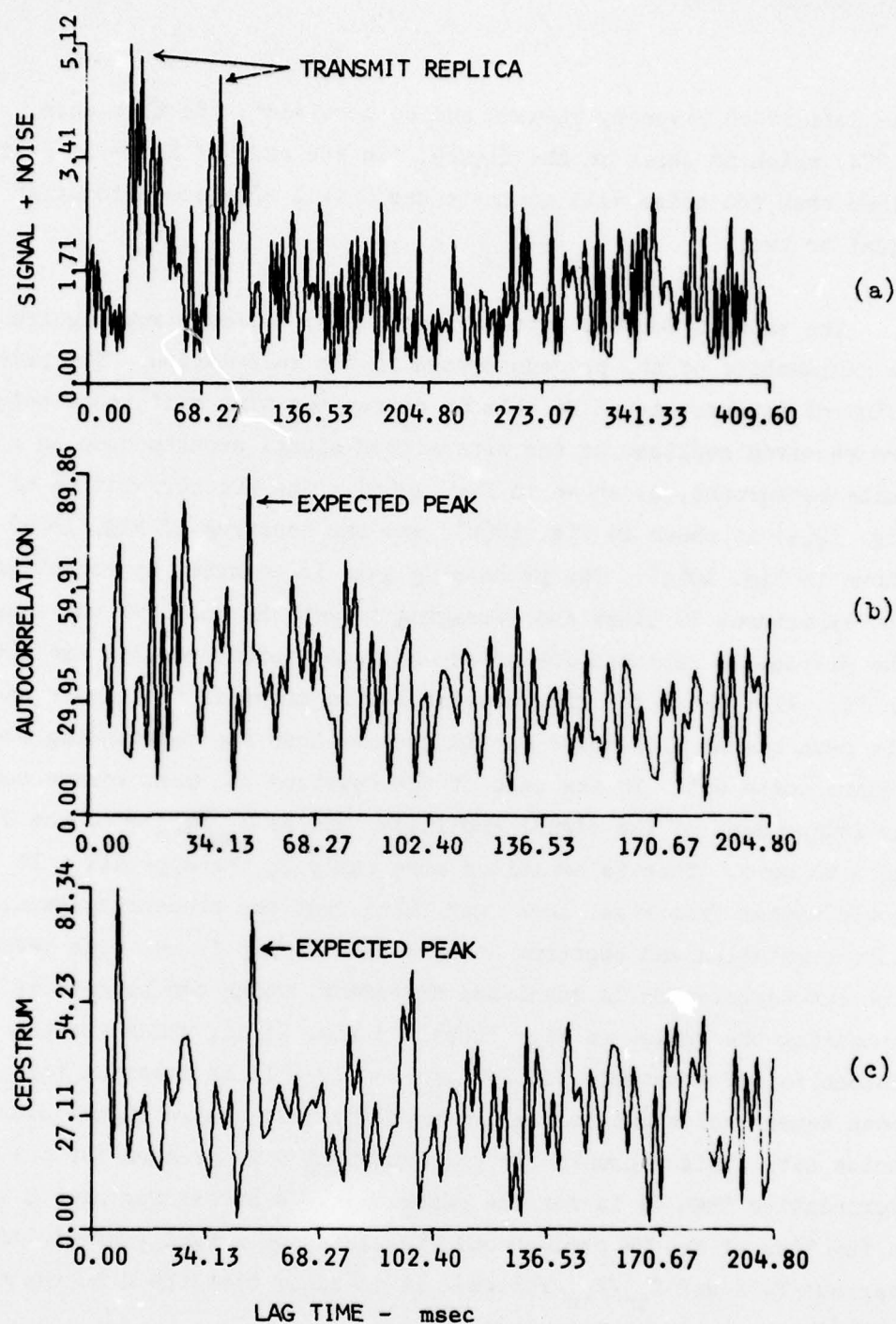


FIGURE 10

SIGNAL PROCESSING ON SIGNAL + NOISE

AS-70-1336

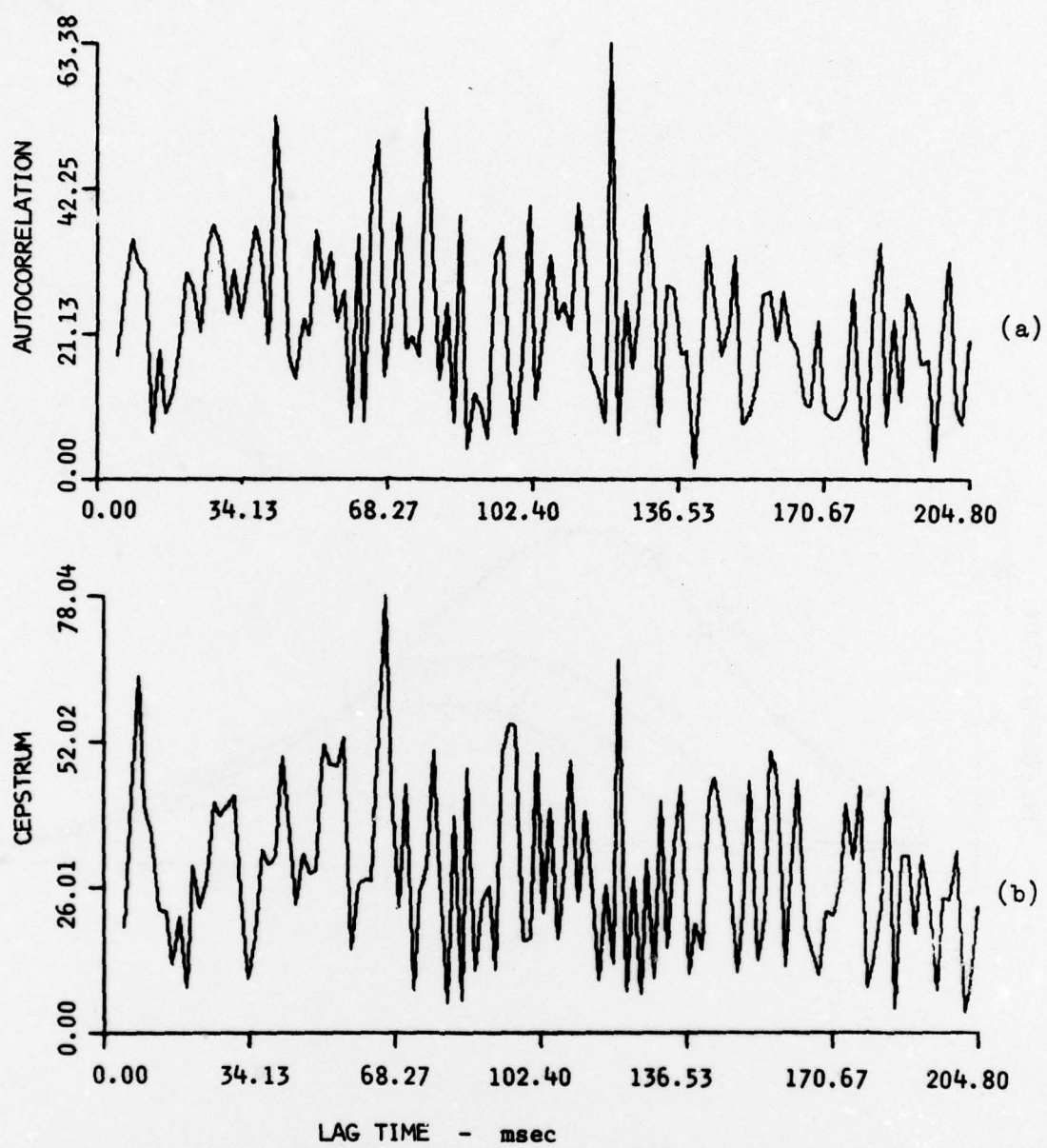


FIGURE 11

SIGNAL PROCESSING ON NOISE ONLY

AS-70-1337

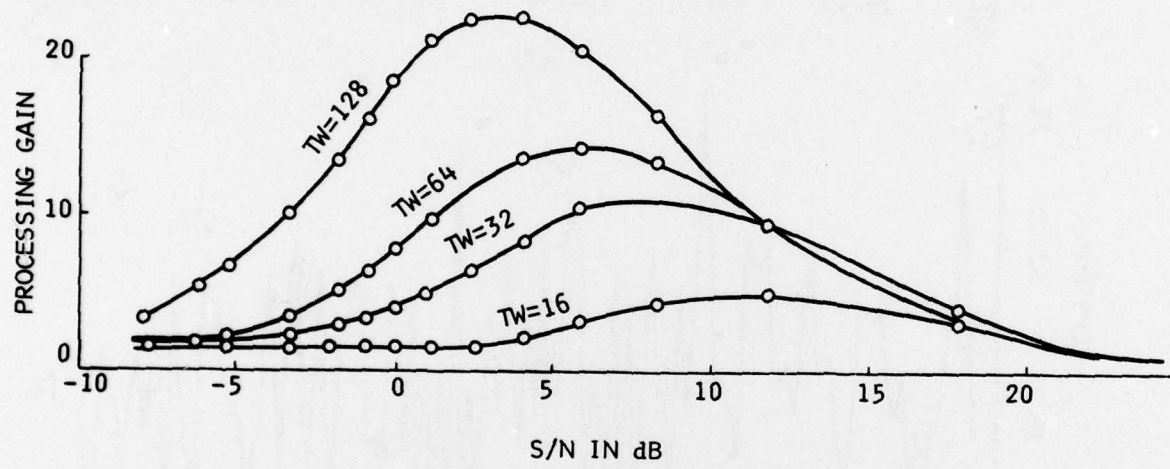


FIGURE 12

PROCESSING GAIN FOR CEPSTRUM

V. COMMENTS

The work that has been done on the processing gain is of real value. For example, the cepstrums of the Lake Travis 3 point data were of large signals superimposed in a low noise background and consequently the cepstrum peaks indicating the target were small. It is now clear that this is true because the processing gain of cepstrum goes to zero as the signal-to-noise ratio goes to infinity. This work will be continued to include the effects of averaging. A crucial point has now been reached in the overall program. If the effect of averaging on cepstrum does not increase the processing gain by several orders of magnitude, then it will be recommended that cepstrum is not suitable for a processor of active sonar return signals. This will be studied in the future.

APPENDIX I

The purpose of this appendix is to find analytically the cepstrum processing gain for the extreme limits of S/N. The processing gain can be defined several different ways,² and in this study it will be defined as

$$G = \frac{\text{Peak}(S+N)_o^2 / N_o}{(S+N)_{in}^2 / N_{in}} , \quad (A-1)$$

where

$\text{Peak}(S+N)_o^2$ = square of (signal + noise) peak out,

N_o = mean square noise out,

$(S+N)_{in}^2$ = mean square signal + noise input, and

N_{in} = mean square noise input.

Cepstrum is a complicated processor and at the present time the function of G is not known analytically as a function of S_{in}/N_{in} , but for the extreme limits of $S_{in}/N_{in} \rightarrow 0$ and $S_{in}/N_{in} \rightarrow \infty$, G can be found.

Let x be a random independent variable normally distributed with mean 0 and variance 1. Then $y=\sigma x$ is a scaled random variable with variance σ^2 . In this case the y represents a noise input to the processor and

$$N_{in} = \frac{1}{M} \sum_{i=1}^M y_i^2 = \frac{1}{M} \sum_{i=1}^M \sigma^2 x_i^2 = \sigma^2 . \quad (A-2)$$

The mean square noise out is a bit more complicated. Let $F\{y\}$ be the Fourier transformation of y . Then the cepstrum of y is

$$Cep = \left| F \left\{ \ln(|F\{y\}|^2) - \text{mean} \right\} \right|^2 , \quad (A-3)$$

where $|F\{y\}|^2 = \sigma^2 |F\{x\}|^2$. Then

$$Cep = \left| F \left\{ \ln \sigma^2 + 2 \ln |F\{x\}| - \text{mean} \right\} \right|^2 . \quad (A-4)$$

It is seen that the mean square of Cep will always be a constant K because subtracting the mean will cancel the effects of $\ln \sigma^2$ and, on the average, $F\{x\}$ will always be the same. That is, $N_o = K$ is a constant. In the limiting case of small signal and large noise, the processing gain becomes

$$\lim_{S/N \rightarrow 0} \text{Est} \left[\frac{\text{Peak}(S+N_o)^2 / N_o}{(S+N)_{in}^2 / N_{in}} \right] = \frac{2K/K}{\sigma^2/\sigma^2} = 2 , \quad (A-5)$$

where it is found that

$$\text{Est}(N_o^2) = \int_0^\infty N_o^2 \chi^2_2(N_o) dN_o = 2K , \quad (A-6)$$

because N_o is a chi-square variate with two degrees of freedom.³

For the case of large signal and small noise, we consider the special case of a received signal r , consisting of two superimposed replicas of the transmitted signal,

$$r(t) = ax(t) + ax(t-\tau) . \quad (A-7)$$

Then the cepstrum of r is found to be

$$C_{ep} = \left| F \left\{ \ln 2a^2 + \ln |F(x)|^2 + \ln(1+\cos\omega\tau) - \text{mean} \right\} \right|^2 , \quad (A-8)$$

$$C_{ep} \approx |F(\cos\omega\tau)|^2 = 1 \text{ (at lag time equal } \tau \text{)} . \quad (A-9)$$

Again it is seen that the cepstrum output is independent of the signal amplitude because of the removal of the mean in the process. Then

$$\lim_{S/N \rightarrow \infty} \text{Est}(G) = \lim_{a^2/\sigma^2 \rightarrow \infty} \left(\frac{1/K}{a^2/\sigma^2} \right) = 0 . \quad (A-10)$$

It is concluded that for small signal and large noise, G approaches 2, and for large signal and small noise, G approaches zero. This has been shown experimentally.

REFERENCES

1. Middleton, David, "Acoustic Modeling, Simulation, and Analysis of Complex Underwater Targets, II. Statistical Evaluation of Experimental Data," Applied Research Laboratories Technical Report No. 70-25 (ARL-TR-70-25), The University of Texas at Austin, 26 June 1969.
2. Steward, J. L., and E. C. Westerfield, "A Theory of Active Sonar Detection," Proceedings from IRE, 44, 872-881 (May 1959).
3. Cramer, Harold, Mathematical Statistics (Princeton University Press, 1946) Section 18.1.

26 October 1970

DISTRIBUTION LIST FOR
QPR No. 3 UNDER N00024-70-C-1184
PROJECT SERIAL No. SF 11121103, TASK 8614
(5 JULY - 5 OCTOBER 1970)
FOR OFFICIAL USE ONLY

Copy No.

- 1 - 4 Commander
Naval Ship Systems Command
Department of the Navy
Washington, D. C. 20360
Attn: SHIPS OOVLC3
- 5 Office of Naval Research
Resident Representative
Lowich Building
1103 Guadalupe
Austin, Texas 78701
- 6 Computer Science Division, ARL/UT
- 7 Signal Physics Division, ARL/UT
- 8 Underwater Missiles Division, ARL/UT
- 9 S. P. Pitt, ARL/UT
- 10 W. W. Ryan, ARL/UT
- 11 R. E. Senterfitt, ARL/UT
- 12 J. A. Shooter, ARL/UT
- 13 Library, ARL/UT